SWIPT-Enabled Relaying in IoT Networks Operating with Finite Blocklength Codes

Yulin Hu, Yao Zhu, M. Cenk Gursoy and Anke Schmeink

Abstract

This paper considers simultaneous wireless information and power transfer (SWIPT) mechanisms in a relaying-assisted ultra-reliable low latency communication network operating with finite blocklength (FBL) codes. The reliability of the network is maximized by the optimal selection of SWIPT parameters under both a power splitting (PS) protocol and a time switching (TS) protocol. In addition, we propose a protocol to improve the reliability performance by introducing a tradeoff between the PS and TS protocols. To further improve the reliability, a joint design is provided, which aligns the optimal selection of SWIPT parameters together with a blocklength allocation between two relaying hops. Via simulations, we validate our analytical model and show that the proposed algorithm achieves the same performance as that obtained with exhaustive search. In addition, we evaluate the considered network, and characterize the impact of blocklength, transmit power and packet size on the reliability of the considered SWIPT-enabled relaying network. Finally, the performance advantages of the proposed protocol (in comparison to the PS and TS protocols) and the proposed joint designs are investigated.

Index Terms

Energy harvesting, finite blocklength, power splitting, relaying, SWIPT, time switching, URLLC.

I. Introduction

Future wireless networks are expected to provide high data rate and low energy consumption while guaranteeing different levels of reliability and latency requirements [1], [2]. In particular, there has recently been significant interest in having wireless links to support ultra reliable and low latency communication (URLLC)[1] services as relevant in several applications in the Internet of Things (IoT) [4] involving, e.g., haptic feedback in virtual/augmented reality, industrial automation, tactile internet, and E-health. A common characteristic of the IoT scenarios is the energy supply limitation, i.e., IoT devices are usually powered by limited battery energy and the batteries are costly or impratical to be replaced regularly [5]. To address this issue, integrating energy harvesting (EH) technologies into communication networks can be applied to prolong the IoT network lifetime [5], [6] by replenishing the energy from various sources, e.g., solar, wind, vibrations, and radio frequency (RF) radiation. Among such energy sources, RF radiation is of particular interest as the source can send signals carrying both energy and information at the same time [7], thus enabling simultaneous wireless information and power transfer (SWIPT). In particular, it has been shown that relay-assisted SWIPT significantly improves the overall transmission performance [8], [9].

Typically, two protocols have been proposed for SWIPT networks [10], namely, power splitting (PS) and time switching (TS). In [11], PS and TS protocols have been applied in relaying networks, by letting the relay harvest energy from the source and then forward the data packet to the destination. The outage probability of a SWIPT-enabled relaying network is determined considering these two protocols in [11]. In addition, the reliability performance has been studied in a multi-user decode-and-forward (DF) relaying network in [12]. The SWIPT performance is studied in [13] under the assumption of imperfect channel information. In [14], the error probability of SWIPT protocols has been investigated in a large-scale relay network. In addition, the outage probability is minimized in [15] subject to a total energy consumption constraint. However, all the above-mentioned studies on the SWIPT-enabled relaying

[1]Different from the specific URLLC traffic defined in 5G [3], in this work the URLLC is a general concept of all types of wireless communications with ultra reliable and low latency requirements.

network are performed under the ideal assumption of communicating arbitrarily reliably at Shannon's channel capacity, i.e., codewords are assumed to be infinitely long.

In the finite blocklength (FBL) regime, i.e., under the assumption of FBL, data transmissions are not arbitrarily reliable. Especially when the blocklength is short, the error probability becomes significant even if the coding rate is below the Shannon limit. Taking this into account, an accurate approximation of the achievable coding rate under the FBL assumption for an additive white Gaussian noise (AWGN) channel was derived in [16] for a single-hop transmission system. Subsequently, the initial work for AWGN channels was extended to Gilbert-Elliott channels [17] and quasi-static fading channels [18], [19]. In our previous work [20]–[22], the FBL performance (the performance level achieved under the FBL assumption) was generally determined for a relaying network without applying SWIPT mechanisms, i.e., the relay does not perform EH and hence consumes its own energy for forwarding data to the destination. On the other hand, it is of much interest to analyze the FBL performance of SWIPT-enabled relaying in a URLLC network, and determine the role of resource overhead for energy transfer and energy loss during the SWIPT process. With such a motivation, the FBL performance of EH and SWIPT network is studied recently. The achievable data rate of a point-to-point transmission with an energy harvesting transmitter was characterized for a noiseless binary communications channel [23]. For a point-to-point SWIPT network, the data rate and delay performance [24], the FBL throughput [25] and the error probability [26] of a point-to-point SWIPT network have been studied. The energy supply probability [27] and the achievable throughput [27], [28] have been addressed for the SWIPT-enabled DF relaying network with FBL codes. The outage probability and the throughput of amplify-and-forward relaying under TS or the PS protocols have been derived in [29]. However, the optimal transmission design, especially the optimal resource allocation, for SWIPT-enabled DF relaying networks under either the TS or the PS protocol has not been addressed so far in the FBL regime.

In this work, we consider a SWIPT-enabled DF relaying network operating with FBL codes, in which the source sends information and energy simultaneously to a relay, and the relay subsequently forwards the received data to D powered by the harvested energy. The relay is assumed to be able to work in both the PS and TS modes. Our aim is to minimize the overall error probability in the FBL regime. The contributions of this paper can be further detailed as follows:

- We determine in the FBL regime the reliability performance of a SWIPT-enabled relaying network considering both PS and TS protocols. Moreover, we provide a design framework to optimize the reliability performance by optimally choosing the SWIPT parameters (either the PS ratio or the TS interval) for these two protocols, after proving the convexity of the corresponding optimization problems. In particular, we show that under the PS protocol the overall error probability is convex in the PS ratio and the blocklength of the first hop of relaying, and also prove that under the TS protocol the overall error probability is convex in the blocklength decisions for the energy harvesting phase and the first hop (data transmission) of relaying.
- Moreover, to further improve the reliability of the considered network, we propose a joint SWIPT protocol which introduces a tradeoff between the PS protocol and the TS protocol. Under the proposed protocol, we also determine the reliability performance in the FBL regime. In particular, an optimal design by scheduling the SWIPT parameters (both the PS ratio or the TS interval) is provided for the proposed tradeoff protocol.
- Furthermore, a joint design on the considered SWIPT-enabled relaying network is then proposed to improve the reliability one step further, which aligns the above optimal selection of SWIPT parameters together with a blocklength allocation between the two hops of relaying.
- Via simulations, we demonstrate the performance advantages of the proposed protocol and identify the impact of coding blocklength and packet size on the reliability of the considered SWIPT-enabled relaying network. In addition, it is shown that the proposed algorithm achieves the same performance as that attained with exhaustive search. Furthermore, the performance advantages of the proposed protocol (in comparison to the PS and TS protocols) and the proposed joint designs are investigated.

The remainder of the paper is organized as follows: In Section II, we describe the system model and briefly provide the background on the FBL regime. In addition, the general problem statements are also provided at the end of the section. In Section III, we first study the PS and TS protocols and minimize the overall error probability in the FBL regime under the two protocols. Subsequently, we propose a joint TP-S protocol and minimize the corresponding overall error probability. To further improve the reliability of the considered network, a joint optimal design is provided in Section IV, where both the SWIPT parameter selection and blocklength allocation between two relaying hops are jointly considered in the design. We provide our simulation results in Section V and finally conclude the paper in Section VI.

II. Preliminaries

In this section, we first describe the system. Subsequently, the FBL performance model of a single hop transmission is reviewed. Finally, we state the problem for minimizing the overall error probability of the considered network.

A. System Description

We study a dual-hop relaying system with a source S, a DF relay R and a destination D, as shown in Fig. 1. A data packet at S with (a potentially considerable size of) k bits needs to be transmitted to D while satisfying URLLC requirements. We consider the scenario [28]–[31] where the channel between S

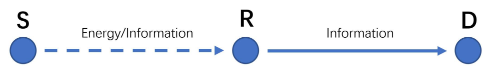

Fig. 1. An example of the considered network.

and D is weak, e.g., the line of sight (LOS) communication is infeasible, and information transfer must rely on R. In particular, S provides energy supply for the transmisison from R to D by applying SWIPT protocols. The system operates in a time-slotted fashion, where time is divided into frames. The length of each frame is $L+M$ symbols, including an initialization period with a length of L symbols and a transmission period with a length of M symbols. The initialization period is used for CSI acquisition and beacon transmission (i.e., including the decision of SWIPT parameter selection and blocklength allocation) while the data (and power) transmission is performed in the transmission period. In addition, each frame corresponds to $T=(L+M)T_{\mathrm{s}}$ seconds, where T_s denotes a symbol duration. In a transmission period, the source is required to transmit the data packet to D with the help of R. Within the transmission period, R first harvests energy and receives information from the source. Our system model follows the proper Gaussian signaling, with which the energy conversion efficiency $\eta \in (0,1)$ is constant in the data coding rate. If R decodes the data packet successfully, it forwards the data packet to D in the subsequent hop using the harvested energy.

We denote by φ_1 and φ_2 the path-losses of the S-R link and the R-D link, respectively. In addition, denote by P_s the transmission power at the source while the noise of the two links are represented by δ_i and with powers σ_i^2, $i=1,2$. Hence, the received signals at R and D can be expressed as

$$y_1 = \sqrt{P_s\varphi_1}x_1h_1 + \delta_1\,, \tag{1}$$

$$y_2 = \sqrt{P_r\varphi_2}x_2h_2 + \delta_2\,, \tag{2}$$

where P_r is the transmit power at R, which is subject to the harvested energy at the R. In addition, x_1 and x_2 are the transmitted signals from R and S. These two signals carry the same data but may be with different blocklengths. Moreover, h_i, $i=1,2$ are the channel coefficients of the two links. The corresponding gains of the two channels are further expressed by $z_i=|h_i|^2$, $i=1,2$. Finally, in this work channels of the two links are assumed to be independent and experience quasi-static fading, i.e., the channel state of each link is constant during one block, and varies independently to the next.

B. FBL performance model of a single-hop transmission

For AWGN channels, [16] derives a tight bound for the coding rate of a single-hop transmission system. With blocklength n, block error probability ε and SNR γ, the coding rate (in bits per channel use) is given by $r = \frac{1}{2}\log_2(1+\gamma) - \sqrt{(1-\frac{1}{(1+\gamma)^2})/2n}Q^{-1}(\varepsilon)\log_2 e + \frac{O(\log_2 n)}{n}$, where $Q^{-1}(\cdot)$ is the inverse of the Q-function given by $Q(w) = \int_w^\infty \frac{1}{\sqrt{2\pi}}e^{-t^2/2}dt$. In [19], the above result has been extended to a complex channel model with received SNR γ, where the coding rate (in bits per channel use) is

$$r = \mathcal{R}(\gamma, \varepsilon, n) \approx \mathcal{C}(\gamma) - \sqrt{\frac{V}{n}} \cdot Q^{-1}(\varepsilon)\,, \tag{3}$$

where $\mathcal{C}(\gamma)$ is the Shannon capacity given by $\mathcal{C}(\gamma) = \log_2(1+\gamma)$. For a complex AWGN channel, $V = \left(1 - \frac{1}{1+\gamma^2}\right)(\log_2 e)^2$ as shown in [19]. Hence, for a single hop transmission with blocklength n and coding rate r, the decoding (block) error probability at the receiver is given by

$$\varepsilon = \mathcal{P}(\gamma, r, n) \approx Q\left(\sqrt{\frac{n}{V}}\,(\mathcal{C}(\gamma) - r)\right). \tag{4}$$

In this paper, we apply the above approximations for investigating the FBL performance of the considered SWIPT system. As these approximations have been shown to be accurate for a sufficiently large value of n [16], for simplicity we will employ them as the rate and error expressions in our analysis. In the following, we first provide the problem statement and subsequently study the FBL performance of SWIPT-enabled two-hop relaying networks.

C. Problem Statement

This work studies the FBL performance of a SWIPT-enabled relaying network. In particular, we are interested in the design of a reliability-optimal system to support URLLC transmissions. On the one hand, code blocklengths of transmission via each link are relatively short. On the other hand, the transmission via each link is required to be reliable enough, i.e., the error probability is lower than a threshold ε_{th}, where in general we assume $\varepsilon_{\text{th}} \ll 10^{-1}$. Recall that the data packet likely has a considerable amount of bits. Hence, it should be mentioned that an ultra reliable transmission cannot be guaranteed if the received SNR at either R or D is extremely low, e.g., $\gamma_i < \gamma_{\text{th}} = 0\,\text{dB}, i = 1, 2$. In the considered work, as both the $\mathrm{S}-\mathrm{R}$ and $\mathrm{R}-\mathrm{D}$ links have the LoS paths, this extremely low SNR case can be ignored, i.e., we assume that $\gamma_i \geq \gamma_{\text{th}} = 0\,\text{dB}, i = 1, 2$ always holds to facilitate the derivations in our analytical model. In the following, we study and optimize the reliability of the considered network.

III. SWIPT Protocols in the FBL Regime: Reliability Analysis and Optimal Design

In this section, we study the FBL performance of a SWIPT-enabled relaying network under the PS protocol, the TS protocol and a proposed joint protocol. In particular, for each protocol, the reliability analysis is conducted first, and subsequently the reliability-optimal SWIPT parameters are characterized.

A. FBL Performance of SWIPT-Enabled Relaying under the PS Protocol

1) Reliability Analysis: As shown in Fig. 2, under the PS protocol, each transmission period consists of two phases corresponding to the two hops of relaying. Each hop/phase has a length of n symbols. The corresponding duration of each phase is given by nT_{s}. Note that the total length of the transmission

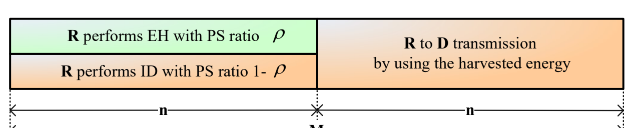

Fig. 2. Frame structure of information/data decoding (IT) and EH in a SWIPT-enabled relaying network under the TS protocol.

period is M symbols, i.e., we have $2n = M$. In addition, the received signal at R in the first phase is split such that a $\rho \in [0, 1]$ fraction of the signal power is used for EH and the remaining $1-\rho$ fraction of the power is used for data packet decoding. Therefore, the SNR of the received split signal at R used for decoding the data packet is given by

$$\gamma_{\mathrm{P},1} = \beta_1(1-\rho)\,, \tag{5}$$

where β_1 is the channel quality indicator of the backhaul link, which does not depend on ρ. It is defined as

$$\beta_1 = \frac{P_s z_1}{\varphi_1 \sigma_1^2}\,. \tag{6}$$

The remainder of the RF power is converted to energy and is harvested by R. The amount of the harvested energy is given by $E_{\mathrm{P}} = nT_{\mathrm{s}}\frac{\eta\rho P_s z_1}{\varphi_1}$, where $\eta \in (0,1)$ is the energy conversion efficiency. Based on the harvested energy, R forwards the packet to D as long as R decodes the data packet successfully. Tthe SNR of the signal received at D in the second phase is

$$\gamma_{\mathrm{P},2} = \frac{E_{\mathrm{P}} z_2}{nT_{\mathrm{s}}\varphi_2\sigma_2^2} = \rho\beta_2\,, \tag{7}$$

where β_2 is channel quality indicator of the relaying link and can be expressed as

$$\beta_2 = \frac{\eta P_s z_1 z_2}{\varphi_1\varphi_2\sigma_2^2}\,. \tag{8}$$

Recall that the packet size is fixed as k. Hence, the coding rate (in bits/symbol) of each phase is given by $r_1 = r_2 = k/n$. According to (4), error probabilities of the first and the second hops are given by $\varepsilon_{\mathrm{P},1} = \mathcal{P}(\gamma_{\mathrm{P},1}, k/n, n)$ and $\varepsilon_{\mathrm{P},2} = \mathcal{P}(\gamma_{\mathrm{P},2}, k/n, n)$, respectively. Then, the overall error probability of the two-hop transmission under PS is

$$\varepsilon_{\mathrm{P,O}} = \varepsilon_{\mathrm{P},1} + (1-\varepsilon_{\mathrm{P},1})\varepsilon_{\mathrm{P},2} = \varepsilon_{\mathrm{P},1} + \varepsilon_{\mathrm{P},2} - \varepsilon_{\mathrm{P},1}\varepsilon_{\mathrm{P},2}\,. \tag{9}$$

It is clear that for a given k and a given n, $\varepsilon_{\mathrm{P},1}$ and $\varepsilon_{\mathrm{P},1}$ are fully determined by $\gamma_{\mathrm{P},1}$, $\gamma_{\mathrm{P},2}$. Note that $\gamma_{\mathrm{P},1}$ and $\gamma_{\mathrm{P},2}$ are functions of ρ. As a result, $\varepsilon_{\mathrm{P},1}$ and $\varepsilon_{\mathrm{P},1}$ as well as $\varepsilon_{\mathrm{P,O}}$ actually are strongly influenced by the choice of ρ.

2) Optimal Design: According to (9), the reliability of the two-hop transmission is determined by $\varepsilon_{\mathrm{P},1}$ and $\varepsilon_{\mathrm{P},2}$ which, as noted above, depend on ρ. Therefore, we provide an optimal design in this subsection to minimize this overall probability by optimally selecting ρ. Recall that we consider a network supporting URLLC transmissions, where the reliability constraint in terms of SNR is given by $\gamma_i \geq \gamma_{\mathrm{th}} \geq 0$ dB, $i = 1, 2$. Hence, the optimization problem under the PS protocol can be stated as follows

$$\begin{aligned} \min_{\rho} \quad & \varepsilon_{\mathrm{P,O}}(\rho) \\ s.t. \quad & \gamma_{\mathrm{P},i} \geq \gamma_{\mathrm{th}}, \qquad i = 1, 2; \\ & 0 < \rho < 1\,. \end{aligned} \tag{10}$$

Then, we provide the following key proposition for solving the Problem (10) .

Proposition 1. *Under the constraint $\gamma_{\mathrm{P},i} \geq 1, i = 1, 2$, for given n, $\varepsilon_{\mathrm{P},1}$ and $\varepsilon_{\mathrm{P},2}$ are convex in ρ, $\rho \in (0,1)$. Under the assumption that each link is sufficiently reliable and the error probability for each link is sufficiently small such that $\varepsilon_{\mathrm{P,O}} \approx \varepsilon_{\mathrm{P},1} + \varepsilon_{\mathrm{P},2}$[2], the overall error probability $\varepsilon_{\mathrm{P,O}}$ of the SWIPT-enabled relaying network with the PS protocol is convex in ρ, $\rho \in (0,1)$.*

Proof. See Appendix A. □

According to Proposition 1, Problem (10) can be efficiently solved by applying convex optimization techniques.

[2]When the error probability for each link is sufficiently small, i.e., $\varepsilon_{\mathrm{P},i} \leq 10^{-1}$, $i = 1, 2$, we have $\varepsilon_{\mathrm{P},1} + \varepsilon_{\mathrm{P},2} \gg \varepsilon_{\mathrm{P},1} \cdot \varepsilon_{\mathrm{P},2}$. Hence, $\varepsilon_{\mathrm{P,O}} \approx \varepsilon_{\mathrm{P},1} + \varepsilon_{\mathrm{P},2}$.

B. FBL Performance of SWIPT-Enabled Relaying under the TS Protocol

In this section, we consider the TS protocol whose structure of the transmission period is shown in Fig. 3.

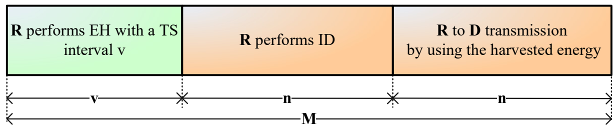

Fig. 3. The structure of the transmission period (including the information/data decoding (ID) and EH) in a SWIPT-enabled relaying network under the TS protocol.

1) Reliability Analysis: As shown in Fig. 3, under the TS protocol each transmission period has three phases, which have blocklengths set as v, n, and n, respectively. In addition, we have $v + 2n = M$. In the first phase, R performs as a pure EH receiver and harvests energy from the source. As the duration of the first phase is vT_s, the energy harvested by R in this phase under the TS protocol is given by

$$E_\mathrm{T} = vT_\mathrm{s}\frac{\eta P_s z_1}{\varphi_1}\,. \tag{11}$$

Subsequently, R receives and decodes the data packet from the source in the second phase. Different from the PS protocol, all the energy of the received signal in the second phase of the TS protocol is used for information/data decoding. The corresponding SNR at R is given by $\gamma_{\mathrm{T},1} = \beta_1 = \frac{P_s z_1}{\varphi_1 \sigma_1^2}$. In other words, R decodes the data based on this SNR $\gamma_{\mathrm{T},1}$. As the blocklength of each relaying hop is $n = \frac{M-v}{2}$, the decoding error probability is given by $\varepsilon_{\mathrm{T},1} = \mathcal{P}(\gamma_{\mathrm{T},1}, \frac{2k}{M-v}, \frac{M-v}{2})$. Therefore, with probability $1 - \varepsilon_{\mathrm{T},1}$ R decodes the packet successfully. Then, it forwards the packet to D in the last phase using the harvested energy E_T. Then, the received SNR at D is

$$\gamma_{\mathrm{T},2} = \frac{E_\mathrm{T} z_2}{nT_\mathrm{s}\varphi_2\sigma_2^2} = \frac{\eta P_s z_1 z_2}{\varphi_1\varphi_2\sigma_2^2}\frac{v}{n} = \beta_2\frac{v}{n} = \beta_2\frac{2v}{M-v}\,, \tag{12}$$

where β_2 is the channel quality indicator introduced in (8).

Therefore, the decoding error probability at D is $\varepsilon_{\mathrm{T},2} = \mathcal{P}(\gamma_{\mathrm{T},2}, \frac{2k}{M-v}, \frac{M-v}{2})$. Finally, the overall error probability of the TS protocol, given by $\varepsilon_{\mathrm{T,O}}$, can be determined based on (9) by replacing $\varepsilon_{\mathrm{P},i}$ by $\varepsilon_{\mathrm{T},i}, i = 1, 2$. Obviously, $\varepsilon_{\mathrm{T,O}}$ is a function of v.

2) Optimal Design: The optimal design for the TS protocol is to minimize $\varepsilon_{\mathrm{T,O}}$ by determining the optimal duration of the TS interval v. Hence, the optimization problem we consider for the TS protocol is

$$\begin{aligned} \min_{v} \quad & \varepsilon_{\mathrm{T,O}}(v) \\ s.t. \quad & \gamma_{\mathrm{T},i} \geq \gamma_\mathrm{th}, \qquad i = 1, 2; \\ & v \in \mathbb{Z}^+, \;\; v \leq M\,. \end{aligned} \tag{13}$$

Proposition 2. *Under the constraint $\gamma_{\mathrm{T},i} \geq 1, i = 1, 2$, $\varepsilon_{\mathrm{T},1}$ and $\varepsilon_{\mathrm{T},2}$ are convex in the TS interval v, $v \in (0, M)$. Under the assumption that $\varepsilon_{\mathrm{T,O}} \approx \varepsilon_{\mathrm{T},1} + \varepsilon_{\mathrm{T},2}$, the overall error probability $\varepsilon_{\mathrm{T,O}}$ is also convex in v, $v \in (0, M)$.*

Proof. See Appendix B. □

Based on the above Proposition 2, the relaxation of Problem (13) can be solved efficiently. We denote the solution of the relaxed problem by $v_0 \in (0, M)$. If v_0 is an integer, then the optimal solution of the original problem provided in (13) is the same, i.e., $v^* = v_0$. However, it is more likely that v_0 is not an integer. Then, by comparing the values of $\varepsilon_{\mathrm{T,O}}$ at the neighboring nearest integers of the optimal solution of the related problem, the solution of Problem (13) can be further determined. In particular, let $v_\mathrm{ceil} = \lceil v_0 \rceil$ and $v_\mathrm{floor} = \lfloor v_0 \rfloor$, where $\lceil\cdot\rceil$ and $\lfloor\cdot\rfloor$ are ceiling and floor functions, respectively. Then, the optimal solution of the original problem is determined by $v^* = \underset{v \in \{v_\mathrm{ceil}, v_\mathrm{floor}\}}{\arg\min}\; \varepsilon_{\mathrm{T,O}}(v)$.

C. Proposed PT-S Protocol

In the previous two subsections, the FBL performances of the SWIPT-enabled relaying network have been addressed under PS and TS protocols. Actually, the key differences between PS and TS protocols in the FBL regime are the following: The PS protocol splits the received power at R and therefore has a lower SNR for decoding the data packet. In comparison to the PS protocol, the TS protocol provides a relatively higher SNR but shorter blocklengths for data transmission, as shown in Fig. 2 and Fig. 3. In other words, these two protocols make different decisions with respect to the tradeoff between the SNR and the blocklength. According to (4), the error probability in the FBL regime is influenced by both the blocklength and the SNR, which is different from the infinite blocklength (IBL) regime where the reliability is only influenced by the SNR for a given coding rate. This motivates us to propose a joint protocol, namely PT-S, to combine the advantages of both PS and TS protocols by striking a balance between reducing the SNR and shortening the blocklength. We show the frame structure of the proposed PT-S protocol in Fig. 4, where both the features of the PS and TS protocols can be found in this tradeoff protocol.

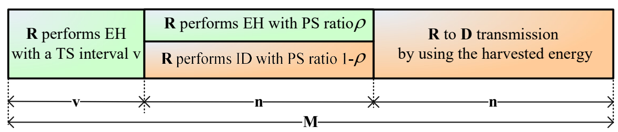

Fig. 4. The structure of the transmission period (including the information/data decoding (ID) and EH in a SWIPT-enabled relaying network under a PT-S protocol.

1) Reliability Analysis: As shown in Fig. 4, each transmission period (with a length of M symbols) under the proposed PT-S protocol is divided into three phases, with lengths v, n and n. Similar to the TS protocol, in the first phase (TS interval) with a length of v, R performs as a pure EH receiver and harvests energy from the source. In other words, the two hops of data transmission (via R) only occur in the second and third phases. In the second phase, R works under the PS protocol with the splitting ratio ρ. Finally, in the last phase, R forwards the packet to D based on the energy harvested in the previous two phases.

Under the proposed PT-S protocol, the energy harvested by R in the first phase is given by $E_{\mathrm{PT},1} = vT_{\mathrm{s}}\frac{\eta P_s z_1}{\varphi_1}$. In the second phase, the energy harvested by R with splitting ratio ρ is given by $E_{\mathrm{PT},2} = nT_{\mathrm{s}}\frac{\eta\rho P_s z_1}{\varphi_1}$. At the same time, the SNR for decoding the data packet at R (in the second phase) actually shares the same expression as (5), i.e., it is given by $\gamma_{\mathrm{PT},1} = \beta_1(1-\rho)$. Note that under the PT-S protocol, each hop of data transmission needs to send k bits via a coding block of length $n = \frac{M-v}{2}$. Hence, the data coding rates of the two hops of relaying are given by $r_1 = r_2 = \frac{k}{n} = \frac{2k}{M-v}$.

The reliability performance of the considered network under the proposed PT-S protocol is determined as follows. In the first hop of data transmission (in the second phase), based on the coding rate $r_1 = \frac{2k}{M-v}$ and the SNR $\gamma_{\mathrm{PT},1}$, the decoding error probability at R is given by $\varepsilon_{\mathrm{PT},1} = \mathcal{P}(\gamma_{\mathrm{PT},1}, \frac{2k}{M-v}, \frac{M-v}{2})$. For the data transmission in the second hop, the energy for transmission is harvested in both the first and second phases. In particular, the total energy harvested by R under the PT-S protocol is $E_{\mathrm{PT}} = E_{\mathrm{PT},1} + E_{\mathrm{PT},2}$. Note that this amount of energy is used by R to forward the data packet (with size k) to D via a block of length n. Hence, the SNR of the received signal at D is given by

$$\begin{aligned}\gamma_{\mathrm{PT},2} &= \frac{E_{\mathrm{PT}} z_2}{nT_{\mathrm{s}}\varphi_2\sigma_2^2} = \frac{\eta P_s z_1 z_2}{\varphi_1\varphi_2\sigma_2^2}\frac{v}{n} + \frac{\rho\eta P_s z_1 z_2}{\varphi_1\varphi_2\sigma_2^2} \\ &= \beta_2\left(\frac{2v}{M-v} + \rho\right).\end{aligned} \tag{14}$$

Based on $\gamma_{\mathrm{PT},2}$ and the coding rate $r_2 = \frac{2k}{M-v}$, the decoding error probability at D is therefore given by $\varepsilon_{\mathrm{PT},2} = \mathcal{P}(\gamma_{\mathrm{PT},2}, \frac{2k}{M-v}, \frac{M-v}{2})$. Hence, the overall error probability $\varepsilon_{\mathrm{PT,O}}$ under the PT-S protocol can be determined by inserting $\varepsilon_{\mathrm{PT},1}$ and $\varepsilon_{\mathrm{PT},2}$ into (9). Therefore, $\varepsilon_{\mathrm{PT,O}}$ is now a function of both v and ρ.

2) Optimal Design: Under the PT-S protocol, the reliability-optimal design becomes a 2-dimensional optimization problem:

$$\begin{array}{ll} \min\limits_{v,\rho} & \varepsilon_{\text{PT,O}}\left(v,\rho\right) \\ s.t. & \gamma_{\text{PT},i}\geq 1, \qquad i=1,2; \\ & v\in\mathbb{Z}^{+}; v\leq M; \\ & 0<\rho<1. \end{array} \tag{15}$$

We next have the following proposition for Problem (15) regarding the relationship between the objective function and the two optimization variables.

Proposition 3. *$\varepsilon_{PT,1}$,$\varepsilon_{PT,2}$ and $\varepsilon_{PT,O}$ of a SWIPT-enabled relaying network under the proposed PT-S protocol are influenced by two parameters, i.e., v, ρ. Under the constraint $\gamma_{\text{PT},i}\geq 1, i=1,2$ and the assumption that $\varepsilon_{\text{PT,O}}\approx\varepsilon_{\text{PT},1}+\varepsilon_{\text{PT},2}$, if one of these two parameters is fixed, $\varepsilon_{PT,1}$,$\varepsilon_{PT,2}$ and $\varepsilon_{PT,O}$ are convex in the other one.*

Proof. See Appendix C. □

According to the above Proposition, problem (15) can be efficiently solved by applying successive convex approximation (SCA) techniques. The key idea is to conduct an iterative search. In particular, we start with an initialized value of v^0 and then have a local problem aiming at minimizing $\varepsilon_{\text{PT,O}}\left(v^0,\rho\right)$ over ρ. We solve this local problem and determine the optimal solution ρ^1 of this problem according to Proposition 3. In the next step, based on ρ^1 we have a new local problem to minimize $\varepsilon_{\text{PT,O}}\left(v,\rho^1\right)$ over v, which can again be efficiently solved according to Proposition 3. Then, we repeat these two steps till the solution converges. The algorithm flow is provided in Algorithm 1 below.

Algorithm 1 : SWIPT Optimization Algorithm for the Proposed PT-S Protocol.

a) Initialize $v^i=M/2$, $i=0$.
b) Solve $\min\limits_{\rho\in(0,1)}\varepsilon_{\text{PT,O}}\left(v^i,\rho\right)$ according to Proposition 3, get solution ρ^{i+1}.
c) Solve $\min\limits_{v\in(0,M)}\varepsilon_{\text{PT,O}}\left(v,\rho^{i+1}\right)$ according to Proposition 3, get solution v^*.
  if v^* is an integer,
    then the optimal solution of the local problem is $v^{i+2}=v^*$.
  else $v^{i+2}=\mathop{\arg\min}\limits_{v\in\{v_{\text{ceil}},v_{\text{floor}}\}}\varepsilon_{\text{PT,O}}\left(v,\rho^{i+1}\right)$, where $v_{\text{ceil}}=\lceil v^*\rceil$ and $v_{\text{floor}}=\lfloor v^*\rfloor$.
d) Repeat the steps b)-c) till the solution converges.

Here, we provide a discussion on the convergence of the above algorithm. Considering the local problem at the i^{th} step, according to the above propositions we have $\min\limits_{\rho}\varepsilon_{\text{PT,O}}\left(v^i,\rho\right)=\varepsilon_{\text{TP,O}}\left(v^i,\rho^{i+1}\right)\geq \min\limits_{v}\varepsilon_{\text{TP,O}}\left(v,\rho^{i+1}\right)\geq\min\limits_{v,\rho}\varepsilon_{\text{P,O}}\left(v,\rho\right)$. Hence, it is easy to show that the optimal value of each local problem is definitely not lower than the optimal value of the original problem provided in (16). According to [32], the convergence of the above algorithm is therefore guaranteed, i.e., at least a local optimum can be achieved. Note that the objective function is smooth and differentiable in (v,ρ) in the feasible set, and that the objective function is convex in v, $\forall\rho\in(0,1)$, and convex in ρ, $\forall v\in\mathbb{Z}^{+}$. Hence, it is easy to show (e.g., via a proof by contradiction) that the local optimum is unique, thus, it is also the global optimum.

IV. Joint Design Combining Blocklength Allocation over Two Relaying Hops

In the previous sections, we have addressed the reliability-oriented optimal design for a SWIPT-enabled relaying network with equal blocklength allocation for the two hops of relaying. In particular, we have minimized the overall error probability for PS, TS and PT-S protocols by optimally selecting the SWIPT parameters, i.e., by determining the optimal PS ratio and/or the optimal TS interval. To further improve the reliability of the network, in this section, we propose a joint design which combines the optimization of the SWIPT parameters (i.e., ρ for PS, v for TS and ρ, v for PT-S) and the coding blocklength allocation between the two hops of relaying.

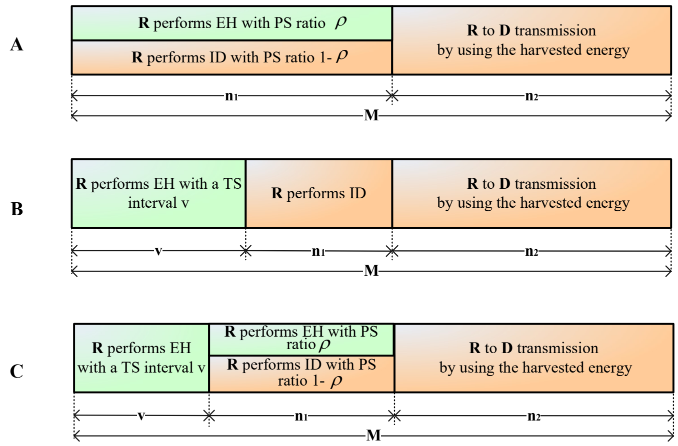

Fig. 5. Frame structures of the considered network with blocklength allocation over two hops of relaying.

A. Joint Design for SWIPT-enabled Relaying under the PS Protocol

As shown in Fig. 5-A, the joint design provides a flexibility to the network where n_1 and n_2 are not necessarily the same, i.e., a certain blocklength allocation can be performed under the length constraint of the transmission period $n_1 + n_2 = M$. Hence, the harvested energy by R is $E_{\mathrm{P}} = n_1 T_{\mathrm{s}} \frac{\eta \rho P_s z_1}{\varphi_1}$. Therefore, the SNR of the signal received at D in the second phase is $\gamma_{\mathrm{P},2} = \frac{E_{\mathrm{P}} z_2}{n_2 T_{\mathrm{s}} \varphi_2 \sigma_2^2} = \frac{n_1}{n_2}\rho\beta_2 = \frac{n_1}{M-n_1}\rho\beta_2$, where β_2 is the channel quality indicator introduced in (8). On the other hand, the coding rate (in bits/symbol) of the two phases are given by $r_1 = \frac{k}{n_1}$ and $r_2 = \frac{k}{n_2} = \frac{k}{M-n_1}$, which result in the corresponding (decoding) error probabilities of the two hops $\varepsilon_{\mathrm{P},1} = \mathcal{P}(\gamma_{\mathrm{P},1}, \frac{k}{n_1}, n_1)$ and $\varepsilon_{\mathrm{P},2} = \mathcal{P}(\gamma_{\mathrm{P},2}, \frac{k}{M-n_1}, M - n_1)$. Finally, the overall error probability $\varepsilon_{\mathrm{P,O}}$ of the two-hop transmission under the PS protocol is obtained from (9). Obviously, $\varepsilon_{\mathrm{P,O}}$ under the joint design is a function of both of ρ and n_1. Here, we provide an optimal joint design to minimize this overall probability by the optimal selection of ρ and n_1. Recall that we consider a network supporting URLLC transmissions, where the reliability constraint in terms of the SNR is given by $\gamma_i \geq \gamma_{\mathrm{th}} \geq 0$ dB, $i = 1, 2$. The optimization problem under the PS protocol is

$$\begin{aligned} \min_{\rho, n_1} \quad & \varepsilon_{\mathrm{P,O}}\left(\rho, n_1\right) \\ s.t. \quad & \gamma_{\mathrm{P},i} \geq \gamma_{\mathrm{th}}, \qquad i = 1, 2; \\ & 0 < \rho < 1; \\ & n_1 \in \mathbb{Z}^+; n_1 \leq M. \end{aligned} \tag{16}$$

To solve the above problem, we first provide the following proposition:

Proposition 4. *Under the constraint $\gamma_{\mathrm{P},i} \geq 1, i = 1, 2$, for a given n_1, $\varepsilon_{\mathrm{P},1}$ and $\varepsilon_{\mathrm{P},2}$ are convex in ρ, $\rho \in (0, 1)$. Again, for sufficiently small error probabilities for each link such that $\varepsilon_{\mathrm{P,O}} \approx \varepsilon_{\mathrm{P},1} + \varepsilon_{\mathrm{P},2}$, the overall error probability $\varepsilon_{\mathrm{P,O}}$ is also convex in ρ, $\rho \in (0, 1)$. In addition, for given ρ, $\varepsilon_{\mathrm{P},1}$, $\varepsilon_{\mathrm{P},2}$ and $\varepsilon_{\mathrm{P,O}} \approx \varepsilon_{\mathrm{P},1} + \varepsilon_{\mathrm{P},2}$ are convex in $n_1 \in (0, M)$.*

Proof. See Appendix D. □

According to the above proposition, problem (16) can be efficiently solved by applying SCA techniques. In particular, Algorithm 1 also holds for solving problem (16) by replacing each local problem of v by the corresponding local problem of n_1, and the convergence is also guaranteed.

B. Joint Design for SWIPT-enabled Relaying under the TS Protocol

As shown in Fig. 5-B, under this joint design, a transmission period under the TS protocol consists of three phases, which have blocklengths of v, n_1, and $n_2 = M - v - n_1$, respectively. The harvested energy and the received SNR at R have the same expressions as in Section III-B, while the decoding error probability at R becomes $\varepsilon_{\mathrm{T},1} = \mathcal{P}(\gamma_{\mathrm{T},1}, \frac{k}{n_1}, n_1)$. In addition, the received SNR at D can be expressed as

$$\gamma_{\mathrm{T},2} = \frac{E_{\mathrm{T}} z_2}{n_2 T_{\mathrm{s}} \varphi_2 \sigma_2^2} = \frac{\eta P_s z_1 z_2}{\varphi_1 \varphi_2 \sigma_2^2} \frac{v}{n_2} = \beta_2 \frac{v}{n_2} = \beta_2 \frac{v}{M - v - n_1} \ , \tag{17}$$

where β_2 is the channel quality indicator introduced in (8). Therefore, the decoding error probability at D is $\varepsilon_{\mathrm{T},2} = \mathcal{P}(\gamma_{\mathrm{T},2}, \frac{k}{M-v-n_1}, M - v - n_1)$. Finally, the overall error probability $\varepsilon_{\mathrm{T,O}}$ can be also determined based on (9). It is clear that $\varepsilon_{\mathrm{T,O}}$ in this joint design can be minimized by determining the optimal values of v and n_1. The optimization problem for the joint design under the TS protocol is given by

$$\begin{aligned} \min_{v,n_1} \quad & \varepsilon_{\mathrm{T,O}}\left(v, n_1\right) \\ s.t. \quad & \gamma_{\mathrm{T},i} \geq \gamma_{\mathrm{th}}, \qquad i = 1, 2; \\ & v, n_1 \in \mathbb{Z}^+; \quad v, n_1 \leq M. \end{aligned} \tag{18}$$

We provide the following proposition for solving the above optimization problem in (18).

Proposition 5. *Under the constraint $\gamma_{\mathrm{T},i} \geq 1, i = 1, 2$, and again the assumption that $\varepsilon_{\mathrm{T,O}} \approx \varepsilon_{\mathrm{T},1} + \varepsilon_{\mathrm{T},2}$, for given n_1, $\varepsilon_{\mathrm{T},1}$, $\varepsilon_{\mathrm{T},2}$ and $\varepsilon_{\mathrm{T,O}}$ are convex in $v \in (0, M - n_1)$. In addition, for given v, $\varepsilon_{\mathrm{T},1}$, $\varepsilon_{\mathrm{T},2}$ and $\varepsilon_{\mathrm{T,O}}$ are also convex in $n_1 \in (0, M - v)$.*

Proof. See Appendix E. □

Based on Proposition 2, Problem (18) can be solved efficiently by applying the SCA algorithm. In particular, Algorithm 1 also holds for the TS protocol by replacing each local problem of ρ by the corresponding local problem of v, and the convergence is also guaranteed.

C. Joint Design for SWIPT-enabled Relaying under the Proposed PT-S Protocol

As shown in Fig. 5-C, within each transmission period under the proposed PT-S protocol, three phases now have lengths v, n_1 and $n_2 = M - v - n_1$, respectively. In comparison to the model discussed in Section III-C, in this joint design the energy harvested by R in the first phase is still given by $E_{\mathrm{PT},1} = v T_{\mathrm{s}} \frac{\eta P_s z_1}{\varphi_1}$ while the energy harvested in the second phase becomes $E_{\mathrm{PT},2} = n_1 T_{\mathrm{s}} \frac{\eta \rho P_s z_1}{\varphi_1}$. Moreover, the error probability in data decoding at R is $\varepsilon_{\mathrm{PT},1} = \mathcal{P}(\gamma_{\mathrm{PT},1}, \frac{k}{n_1}, n_1)$. Note that the total energy harvested by R under the PT-S protocol is $E_{\mathrm{PT}} = E_{\mathrm{PT},1} + E_{\mathrm{PT},2}$, which is used at R to forward the data packet to D via a coding block of length $n_2 = M - v - n_1$. Hence, the SNR of the received signal at D is given by

$$\begin{aligned} \gamma_{\mathrm{PT},2} &= \frac{E_{\mathrm{PT}} z_2}{n_2 T_{\mathrm{s}} \varphi_2 \sigma_2^2} = \frac{\eta P_s z_1 z_2}{\varphi_1 \varphi_2 \sigma_2^2} \frac{v}{n_2} + \frac{\rho \eta P_s z_1 z_2}{\varphi_1 \varphi_2 \sigma_2^2} \\ &= \beta_2 \left(\frac{v}{M - v - n_1} + \frac{n_1}{M - v - n_1} \rho \right). \end{aligned} \tag{19}$$

Further, the error probability at D is $\varepsilon_{\mathrm{PT},2} = \mathcal{P}(\gamma_{\mathrm{PT},2}, \frac{k}{M-v-n_1}, M - v - n_1)$. As a result, the overall error probability $\varepsilon_{\mathrm{PT,O}}$ under the PT-S protocol can be determined according to (9).

Obviously, under this joint design $\varepsilon_{\mathrm{PT,O}}$ is now a function of v, ρ and n_1. Therefore, this reliability-optimal design requires the solution of the following 3-dimensional problem

$$\begin{aligned} \min_{v,\rho,n_1} \quad & \varepsilon_{\mathrm{PT,O}}\left(v, \rho, n_1\right) \\ s.t. \quad & \gamma_{\mathrm{PT},i} \geq 1, \qquad i = 1, 2; \\ & v, n_1 \in \mathbb{Z}^+, \quad v, n_1 \leq M; \\ & \rho \in (0, 1). \end{aligned} \tag{20}$$

We next have the following proposition addressing the optimization problem in (20) regarding the relationship between the objective function and the three optimization variables.

Proposition 6. *The overall error probability $\varepsilon_{PT,O}$ of a SWIPT-enabled relaying network under the proposed PT-S protocol is influenced by three parameters, i.e., v, ρ, n_1. Under the constraint $\gamma_{PT,i} \geq 1, i = 1, 2$ and the assumption that $\varepsilon_{\mathrm{PT,O}} \approx \varepsilon_{\mathrm{PT,1}} + \varepsilon_{\mathrm{PT,2}}$, if two of these three parameters are fixed, $\varepsilon_{PT,O}$ is convex in the third one.*

Proof. See Appendix F. □

According to Proposition 4, Problem (20) can be also solved by SCA algorithms. We provide the flow of the algorithm in Algorithm 3 on the next page. The feasibility of applying the SCA algorithm and the convergence guarantee follow the same arguments as in the discussion provided for Algorithm 1.

Algorithm 2 : Joint Design Algorithm for the proposed PT-S Protocol.

a) Initialize $n_1^i = M/2$ and $\rho^i = 0.5$, $i = 0$.
b) Solve $\min\limits_{v \in (0, M-n_1)} \varepsilon_{\mathrm{P,O}}\left(v, \rho^i, n_1^i\right)$ according to Proposition 3, denote the solution by v^{i+1}.
  if v^* is an integer,
    then optimal solution of the local problem is $v^{i+1} = v^*$.
  else $v^{i+1} = \arg\min\limits_{v \in \{v_{\mathrm{ceil}}, v_{\mathrm{floor}}\}} \varepsilon_{\mathrm{PT,O}}\left(v, \rho^i, n_1^i\right)$, where $v_{\mathrm{ceil}} = \lceil v^* \rceil$ and $v_{\mathrm{floor}} = \lfloor v^* \rfloor$.
c) Solve $\min\limits_{\rho \in (0,1)} \varepsilon_{\mathrm{PT,O}}\left(v^{i+1}, \rho, n_1^i\right)$ according to Proposition 6, have solution ρ^{i+2}.
d) Solve $\min\limits_{n_1 \in (1, M-v^{i+1})} \varepsilon_{\mathrm{PT,O}}\left(v^{i+1}, \rho^{i+2}, n_1\right)$ according to Proposition 6, have solution by n_1^*.
  if n_1^* is an integer,
    then optimal solution of the local problem is $n_1^{i+3} = n_1^*$.
  else $n_1^{i+3} = \arg\min\limits_{n_1 \in \{n_{1,\mathrm{ceil}}, n_{1,\mathrm{floor}}\}} \varepsilon_{\mathrm{TP,O}}\left(v^{i+1}, \rho^{i+2}, n_1\right)$, where $n_{1,\mathrm{ceil}} = \lceil n_1^* \rceil$ and $n_{1,\mathrm{floor}} = \lfloor n_1^* \rfloor$.
e) Repeat the steps b)-d) till the solution converges.

So far, we have proposed the instantaneous designs on SWIPT parameter selection in Section III and the joint design (combining the SWIPT parameter selection with the blocklength allocation over the two relay hops) in Section IV for the considered SWIPT network in the FBL regime. It is worth mentioning that the TS protocol and the proposed PT-S (both with only SWIPT parameter selection) address a similar tradeoff with the joint design, i.e., the tradeoff between EH and data transmission. In particular, the joint design directly makes the tradeoff by allocating blocklengths for EH and data transmission. In addition, the TS and PT-S protocols (without blocklength allocation over the two relay hops) address this tradeoff by adjusting the TS factor v, which influences also the blocklength (given by $\frac{M-v}{2}$) for the data transmission at each hop of relaying. Hence, applying the joint design is expected to result in less improvement in reliability for the TS and PT-S protocols in comparison to the PS one.

V. Numerical Results and Discussion

In this section, we resort to Monte Carlo simulations to confirm the accuracy of our analytical model and evaluate the system performance. We first investigate the reliability achieved by optimally selecting SWIPT parameters of the PS, TS and the proposed PT-S protocols. Subsequently, we study the performance improvements by further considering the blocklength allocation between the two relaying hops. In the simulations, we consider the following parameterization mainly adopted from [25], [28]: Firstly, the transmission power at the source is set to $P_s = 1$ Watt. Secondly, noise powers of the two links are set to $\sigma_1^2 = \sigma_2^2 = 0.01$. In addition, the energy conversion efficiency is set to $\eta = 0.5$. Moreover, the path-losses are obtained based on $\varphi_i = d_i^{-2.7}$, $i = 1, 2$, where d_1 and d_2 are the distances of the two links $d_1 = 1.5$ m and $d_2 = 5$ m. Finally, we consider the Rician quasi-static channel fading with the Rician factor $K = 1$, i.e., the power in the LOS path and the power in the other scattered paths are balanced.

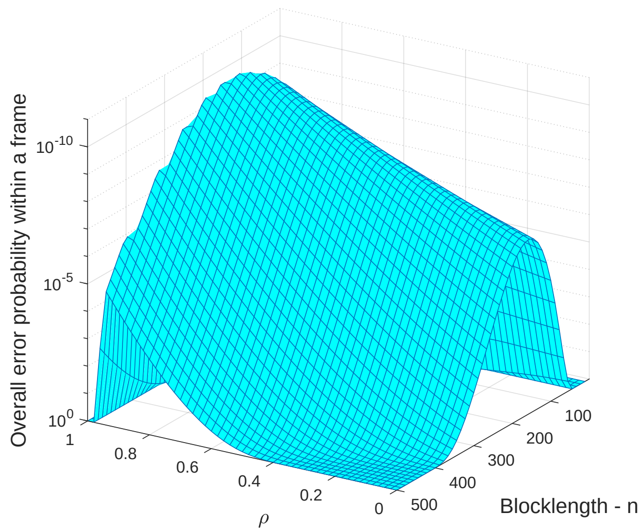

Fig. 6. Error probability ε vs. n and ρ, while packet size is set to 150 bits.

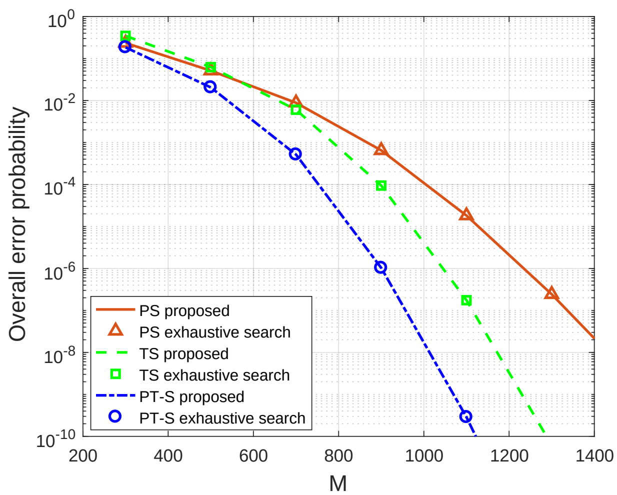

Fig. 7. Reliability achieved by optimally scheduling SWIPT parameters, i.e., PS ratio ρ or/and TS interval v.

A. *Optimal selection of SWIPT parameters*

We start with the investigation on the impact of ρ and n on the overall error probability (within a frame) under the proposed PT-S protocol. The numerical results are provided in Fig. 6. In this simulation, we set $M = 1000$ symbols in the figure, and vary the blocklength n of each hop of relaying and ρ. First of all, the figure demonstrates that the overall error probability is convex in n and ρ in the reliable region (e.g., the error probability is lower than 10^{-1}). Note that as M is fixed, $v = M - 2n$ is affine in n, and vice versa. The figure actually indicates that the overall error probability is also convex in v. These results exactly confirm Proposition 3. Moreover, recall that both the PS and TS protocols can be seen as two specific cases of the PT-S protocol, the performance of the PS and TS protocols can also be observed from the figure. In particular, the performance of the PS protocol can be observed from the curve as ρ varies at point $n = M/2 = 500$, i.e., the left-side edge of the surface. It can seen that when $n = 500$, the overall error probability is convex in ρ, which is predicted by Proposition 1. On the other hand, the right-side edge of the surface, i.e., the curve at $\rho = 0$ is actually the performance of the TS protocol. This curve shows that the overall error probability under the TS protocol is convex in n. As $v = M - 2n$ and M is fixed, this curve actually indicates that the overall error probability is convex in v, which confirms Proposition 2.

Next, we study the impact of the length of the transmission period M on the overall error probability averaged over channel fading, where the proposed optimal SWIPT parameter selection is performed at

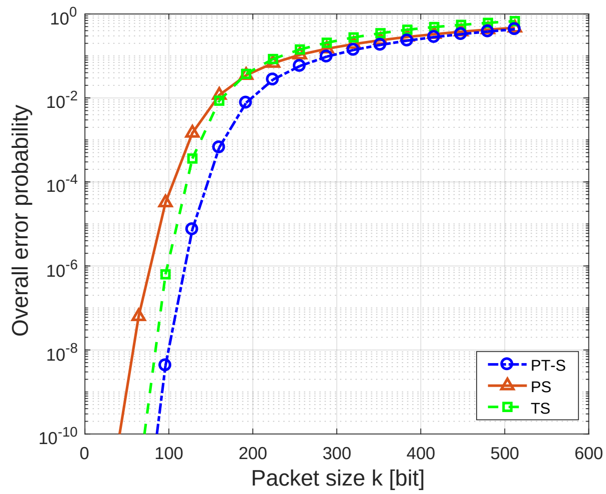

Fig. 8. The impact of packet size k on the overall error probability.

each channel realization. In particular, we evaluate the overall error probability under these three protocols by applying optimization techniques (i.e., backtracking line search) according to Algorithms 1 and 2 while also providing the results obtained by applying exhaustive search as performance benchmarks. The results are shown in Fig. 7. We observe that for each protocol the proposed algorithm achieves the same performance as exhaustive search (which in general has significantly high complexity), which verifying again the accuracy of our analysis. In addition, all the curves decrease as the M increases. More importantly, it can be observed that the proposed PT-S protocol outperforms both the PS and the TS protocols, demonstrating that the PT-S protocol achieves a better tradeoff between the SNR and the blocklength in minimizing the overall error probability. In particular, the performance advantage of the PT-S protocol become more significant as M increases, i.e., achieving an ultra-reliable requirement with a shorter blocklength in comparison to the PS and TS protocols. Moreover, in comparison to the PS protocol, the TS protocol is more reliable for long blocklength scenarios, while the PS protocol is preferred over the TS scheme when the blocklength is quite short.

We next investigate the impact of the packet size of k bits on the reliability performance (also the average reliability over channel fading) in Fig. 8. As expected, a bigger packet size results in a higher error probability for all the three protocols. In addition, the PT-S protocol shows again the reliability advantage in comparison to the TS protocol and the PS protocol. When comparing the PS protocol with the TS scheme, we find that the TS protocol is preferred when the packet is small. On the other hand, the PS protocol has a better reliability performance in the regime of relatively large packet sizes.

B. The performance improvement by the joint design

In the previous subsection, we have investigated in the FBL regime the optimal reliability performances achieved by SWIPT parameter optimization. In the following, we focus on the performance of the joint design which considers both the SWIPT parameter optimization and the blocklength allocation between two relaying hops. We first validate the analytical model of the proposed joint design for the PS, TS and PT-S protocols as well as Propositions 4, 5 and 6. Subsequently, we illustrate the performance improvement by the joint design, i.e. the additional degrees-of-freedom/flexibility introduced by the blocklength allocation between relaying hops.

In Fig. 9 and Fig. 10, we provide under the joint design the overall error probability results of the PS and TS protocols, respectively. Fig. 9 shows that in the joint design for the PS protocol the instantaneous overall error probability is convex in ρ and n_1 in the reliable region (e.g., the error probability is lower than 10^{-1}), which confirms Proposition 4. In addition, Fig. 10 agrees with the characterization in Proposition 5 that the instantaneous overall error probability of the TS protocol in the reliable region is convex in v and n_1, respectively. Moreover, Proposition 6 describes the relationship between the overall error probability of the PT-S protocol in the joint design over parameters ρ, v and n_1. However, this 4-dimensional relationship cannot be illustrated by a 3-dimensional figure, unlike for Propositions 4 and 5. To verify Proposition 6, we have studied the overall error probability by setting different values for either v or ρ and obtained two sets of convex surfaces. Due to the page limitations, these two groups of results are not included in the paper, but it should be mentioned that the surfaces obtained by varying the values of ρ (for fixed values of v) share a similar shape with Fig. 9 while the ones for fixed values of ρ are similar to Fig. 10.

Next, by applying the proposed joint design during each frame, we obtained the reliability performance (over channel fading) for all the three protocols. The results are shown in Fig. 11 where the corresponding performances achieved by applying exhaustive search are also provided. First of all, the figure illustrates that both the proposed algorithms and the exhaustive search achieve the same performance for the considered network operating with the joint design. Secondly, in comparison to Fig. 7 where the PT-S protocol has a significant performance advantage over the PS and TS protocols, the gap between the PT-S protocol and the other two protocols are relatively short owing to the joint design as shown in Fig. 11.

To further investigate the impact of the joint design on these protocols, we provide in Fig. 12 a set of comparisons between purely applying optimal SWIPT parameter selection and the joint design. From the figure, it is easy to notice the performance improvement (for each protocol) by applying the

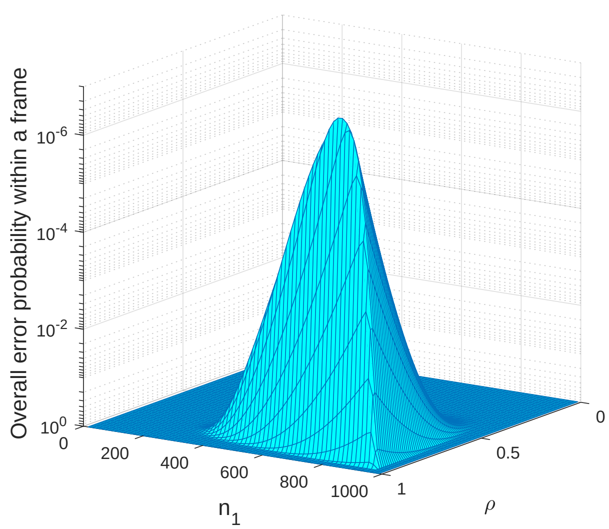

Fig. 9. How in the joint design ρ and n_1 influence the overall error probability (within a frame) under the PS protocol. In the figure, we set $k = 150$ bits and $M = 1000$ symbols.

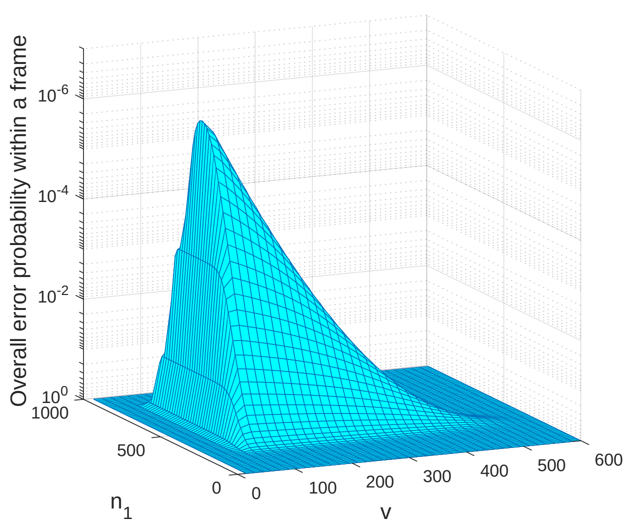

Fig. 10. How in the joint design v and n_1 influence the overall error probability (within a frame) under the TS protocol. In the figure, we set $k = 150$ bits and $M = 1000$ symbols.

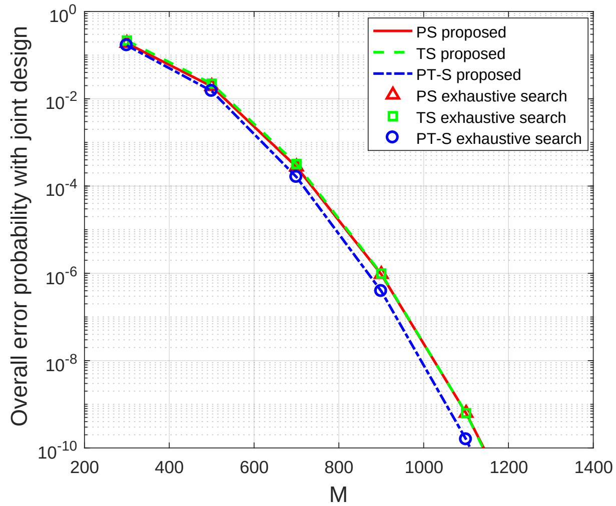

Fig. 11. The average reliability performance (over channel fading) achieved by the joint design.

joint design in comparison to purely optimizing the SWIPT parameters. In general, the performance improvements are relatively more significant when M is large for all protocols. On the other hand, the reliability improvements by applying the joint design are not the same for different protocols. In particular, the reliability improvements for the TS and PT-S protocols are relatively less in comparison to the one for the PS protocol. In particular, this improvement for the PT-S protocol is even tinier than for the TS protocol, as by selecting ρ and υ the PT-S protocol already achieves an excellent tradeoff between EH and data transmission. These observations confirm our discussion at the end of Section IV.

VI. CONCLUSION

In this paper, we have investigated the reliability performance of a SWIPT-enabled relaying network in the FBL regime. We have provided a three-step design to improve the reliability of the network. First, we have considered the PS and the TS protocols and minimized the overall error probability of the network by optimally choosing the SWIPT parameters, PS ratio ρ and TS interval υ. Secondly, we have shown that in the FBL regime there is a tradeoff between the SNR and the blocklength, while both of them influence the reliability. Then, we have proposed the PT-S protocol to improve the reliability by achieving a better tradeoff (than the PS and TS protocols). In addition, to improve the reliability one step further, we have proposed a joint design combining both the SWIPT parameter optimization with blocklength allocation between the two hops of relaying.

Via simulations, we have verified the accurateness of our analytical characterizations. In addition, we have observed that the proposed algorithms achieve the same performance as exhaustive search. More importantly, we have demonstrated the performance advantage of the proposed PT-S protocol in comparison to the TS and the PS protocols. Moreover, we have determined that in comparison to the PS protocol, the TS protocol is more reliable under long blocklength and small packet size scenarios. Furthermore, the joint parameter optimization and blocklength allocation lead to a significant reliability improvement for the PS protocol and a considerable improvement for the TS protocol but a tiny improvement for the proposed PT-S protocol. In particular, (although the proposed PT-S outperforms PS and TS protocols under the scenario with only SWIPT parameter selection) applying the joint design reduces the performance gap between these protocols. This indicates that similar and excellent tradeoff performances, i.e., between the blocklength and the SNR, have been achieved by applying the proposed PT-S protocol and by applying the PS or TS protocols with the proposed joint design. As the tradeoff is addressed from different perspectives but converged to a similar performance is observed, this also indicates that these results are close to the reliability bound which can be achieved by balancing the blocklength and the SNR. Our study suggests the enabling of the relay node to operate using the PT-S protocol, as the PT-S protocol definitely leads to a better performance than the PS and TS protocols. On

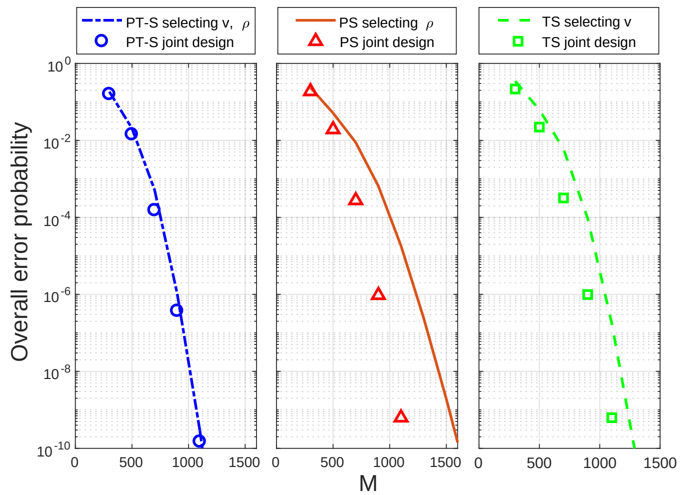

Fig. 12. Performance improvement by a joint design in comparison to purely optimally selecting SWIPT parameters.

$$\frac{\partial^2 w_{\mathrm{P},i}}{\partial \rho^2} = \frac{\beta_i^2}{\sqrt{\frac{V(\gamma_{\mathrm{P},i})}{n_i}}(\gamma_{\mathrm{P},i}^2 - r_i + 1)^2}\left(\left(\frac{3\log_e 2}{((\gamma_{\mathrm{P},i}+1)^2-1)^2} + \frac{3\log_e 2}{((\gamma_{\mathrm{P},i}+1)^2-1)}\right)(\mathcal{C}(\gamma_{\mathrm{P},i}) - r_i) - 1 - \frac{2}{(\gamma_{\mathrm{P},i}+1)^2-1}\right) \tag{22}$$

the other hand, when the joint design is considered and the corresponding additional costs (i.e., cost for synchronization and transmitting the blocklength allocation decision and relatively high computational complexity for solving the joint design problem) are taken into account, the relay operating in a single mode (PS or TS) could also provide a competitive reliability performance.

In this work we provided reliability-oriented designs for a SWIPT-enabled relaying network with a linear energy harvester. It is worth mentioning that recent studies [33]–[36] have shown that a non-linear EH model is more practical and actually introduces a tradeoff between EH and data decoding. This tradeoff can be addressed by considering signalling designs. The reliability performance model and optimal design combining the signalling with SWIPT parameter selection and blocklength allocation are also interesting and open research issues in both the IBL and FBL regimes.

Appendix A
Proof of Proposition 1

We prove the proposition by showing the second order derivatives of $\varepsilon_{\mathrm{P},1}$, $\varepsilon_{\mathrm{P},2}$ and $\varepsilon_{\mathrm{P,O}}$ with respect to ρ are non-negative. To facilitate the proof, we denote $w_{\mathrm{P},i}(\gamma_{\mathrm{P},i}) = \frac{\mathcal{C}(\gamma_{\mathrm{P},i})-r_i}{\sqrt{V(\gamma_{\mathrm{P},i})/n_i}}$. Then, according to (4), for link i, for $i=1,2$, we have

$$\frac{\partial^2 \varepsilon_{\mathrm{P},i}}{\partial \rho^2} = \frac{1}{\sqrt{2\pi}}\exp\left(-\frac{w_{\mathrm{P},i}^2}{2}\right)\left(w_{\mathrm{P},i}\left(\frac{\partial w_{\mathrm{P},i}}{\partial \rho}\right)^2 - \frac{\partial^2 w_{\mathrm{P},i}}{\partial \rho^2}\right). \tag{21}$$

Hence $\frac{\partial^2 \varepsilon_{\mathrm{P},i}}{\partial \rho^2} \geq 0$ if $\frac{\partial^2 w_{\mathrm{P},i}}{\partial \rho^2} \leq 0$. In addition, we can obtain $\frac{\partial^2 w_{\mathrm{P},i}}{\partial \rho^2}$, which given in (22).

Hence, $\frac{\partial^2 w_{\mathrm{P},i}(\gamma_{\mathrm{P},i})}{\partial \rho^2} \leq 0$, if the following condition holds

$$3\log_e 2(\mathcal{C}(\gamma_{\mathrm{P},i}) - r_i) \geq (\gamma_{\mathrm{P},i}+1)^2 - 1\ . \tag{23}$$

It is easy to show $(\gamma_{\mathrm{P},i}+1)^2-1 \geq 3\log_e 2\cdot\mathcal{C}(\gamma_{\mathrm{P},i}) \geq 3\log_e 2(\mathcal{C}(\gamma_{\mathrm{P},i})-r_i)$, $\forall\ \gamma_{\mathrm{P},i} \geq 1 = 0$ dB. Therefore, $\frac{\partial^2 \varepsilon_{\mathrm{P},i}}{\partial \rho^2} \geq 0$, $i=1,2$.

Note that the blocklengths of the two hops are fixed and that the two channels are independent of each other. Then, we have the second derivative of $\varepsilon_{\mathrm{P,O}}$ with respect to ρ given as follows:

$$\frac{\partial^2 \varepsilon_{\mathrm{P,O}}}{\partial \rho^2} \approx \frac{\partial^2 \varepsilon_1}{\partial \rho^2} + \frac{\partial^2 \varepsilon_2}{\partial \rho^2} \ . \tag{24}$$

As a result, $\frac{\partial^2 \varepsilon_{\mathrm{P,O}}}{\partial \rho^2} \geq 0$ holds.

Appendix B
Proof of Proposition 2

Similar to the proof of Proposition 1, here we prove Proposition 2 by showing the second order derivatives of $\varepsilon_{\mathrm{T},i}, i = 1, 2$ in v are non-negative. We introduce $w_{\mathrm{T},i} = \frac{\mathcal{C}(\gamma_{\mathrm{T},i}) - r}{\sqrt{V(\gamma_{\mathrm{T},i})/n}}$. Then, we have $\varepsilon_{\mathrm{T},i} = Q(w_{\mathrm{T},i})$. Note that $v = M - 2n$ and M is a constant. Then, the second derivative of $\varepsilon_{\mathrm{T},i}$ with respect to v is given by

$$\begin{aligned} \frac{\partial^2 \varepsilon_{\mathrm{T},i}}{\partial v^2} &= 4\frac{\partial^2 \varepsilon_{\mathrm{T},i}}{\partial n^2} = 4\frac{\partial^2 \varepsilon_{\mathrm{T},i}}{\partial w_{\mathrm{T},i}^2}\left(\frac{\partial w_{\mathrm{T},i}}{\partial n}\right)^2 + 4\frac{\partial \varepsilon_{\mathrm{T},i}}{\partial w_{\mathrm{T},i}}\frac{\partial^2 w_{\mathrm{T},i}}{\partial n^2} \\ &= \frac{4}{\sqrt{2\pi}} e^{-\frac{w_{\mathrm{T},i}^2}{2}} \left(w_{\mathrm{T},i}\left(\frac{\partial w_{\mathrm{T},i}}{\partial n}\right)^2 - \frac{\partial^2 w_{\mathrm{T},i}}{\partial n^2}\right) . \end{aligned} \tag{25}$$

It is clear that $\frac{\partial^2 \varepsilon_{\mathrm{T},i}}{\partial v^2} \geq 0$ holds if $\frac{\partial^2 w_{\mathrm{T},i}}{\partial n^2} \leq 0$. In the following, we analyze $\frac{\partial^2 w_{\mathrm{T},1}}{\partial n^2}$ and $\frac{\partial^2 w_{\mathrm{T},2}}{\partial n^2}$ in more detail.

For the first hop of relaying, we have $\frac{\partial w_{\mathrm{T},1}}{\partial n} = \frac{C(\gamma_{\mathrm{T},1})n + k}{2n^2\sqrt{\frac{V(\gamma_{\mathrm{T},1})}{n}}} \geq 0$ and the second derivative $\frac{\partial^2 w}{\partial n^2}$ is further given by

$$\frac{\partial^2 w_{\mathrm{T},1}}{\partial n^2} = -\frac{C(\gamma_{\mathrm{T},1})n + 3k}{2n^3\sqrt{V(\gamma_{\mathrm{T},1})/n}} \leq 0 \ . \tag{26}$$

Therefore, we have $\frac{\partial^2 \varepsilon_{\mathrm{T},1}}{\partial v^2} \geq 0$.

For the second hop of relaying, the first derivative of $w_{\mathrm{T},2}$ with respect to n is

$$\begin{aligned} \frac{\partial w_{\mathrm{T},2}}{\partial n} =& \frac{\log_{\mathrm{e}} 2 \left(\frac{-\frac{\beta_2 v}{n^2} + \frac{2\beta_2}{n}}{(\beta_2 \frac{v}{n} + 1)} + \frac{k}{n^2} \right)}{\sqrt{\frac{V(\gamma_{\mathrm{T},1})}{n}}} \\ & - \frac{\log_{\mathrm{e}} 2 \left(\frac{2\left(-\beta_2 \frac{v}{n^2} - \frac{2\beta_2}{n}\right)}{n(\gamma_{\mathrm{T},2}+1)^3} - \frac{V(\gamma_{\mathrm{T},2})}{n^2} \right) \left(C - \frac{k}{n}\right)}{2\left(\frac{V(\gamma_{\mathrm{T},2})}{n}\right)^{\frac{3}{2}}} \ . \end{aligned} \tag{27}$$

In addition, the second derivative is given by

$$\frac{\partial^2 w_{\mathrm{T},2}}{\partial n^2} = \sqrt{\frac{n}{V(\gamma_{\mathrm{T},2})}} \left(A_1 + A_2(C(\gamma_{\mathrm{T},2}) - r)\right) \ , \tag{28}$$

where A_1 and A_2 are given by (29) and (29) on the next page.

To show that A_1 is negative, we reformulate A_1 by

$$A_1 = B_4\beta_2^4 + B_3\beta_2^3 + B_2\beta_2^2 + B_1\beta_2 \ , \tag{31}$$

where

$$
\begin{aligned}
A_1 = &-\frac{\left(2\beta_2 M + n\left(\left(\frac{\beta_2(M-2n)}{n}+1\right)^2-1\right)\left(\frac{\beta_2(M-2n)}{n}+1\right)\right)\left(\beta_2 M - k\log_{\mathrm{e}} 2\cdot\left(\frac{\beta_2(M-2n)}{n}+1\right)\right)}{n^4(\gamma_{\mathrm{T},2}+1)^2((\gamma_{\mathrm{T},2}+1)^2-1)} \\
&-\frac{\left(\left(\frac{\beta_2(M-2n)}{n}+1\right)^2-1\right)\left({\beta_2}^2M^2-2\beta_2 Mn\left(\frac{\beta_2(M-2n)}{n}+1\right)+2k\log_{\mathrm{e}} 2n\left(\frac{\beta_2(M-2n)}{n}+1\right)^2\right)}{n^4(\gamma_{\mathrm{T},2}+1)^2((\gamma_{\mathrm{T},2}+1)^2-1)} .
\end{aligned}
\tag{29}
$$

$$
A_2 = \frac{1}{n^4(\gamma_{\mathrm{T},2}+1)^2((\gamma_{\mathrm{T},2}+1)^2-1)^2}
\left(
\begin{array}{l}
3{\beta_2}^2M^2\left(\left(\frac{\beta_2(M-2n)}{n}+1\right)^2-1\right) \\
-3{\beta_2}^2M^2-\frac{3n^2\left(\left(\frac{\beta_2(M-2n)}{n}+1\right)^2-1\right)^2\left(\frac{\beta_2(M-2n)}{n}+1\right)}{4} \\
-n^2\left(\left(\frac{\beta_2(M-2n)}{n}+1\right)^2-1\right)^2\left(\frac{\beta_2(M-2n)}{n}+1\right)^2 \\
-2\beta_2 Mn^2\left(\left(\frac{\beta_2(M-2n)}{n}+1\right)^2-1\right)\left(\frac{\beta_2(M-2n)}{n}+1\right)^2 \\
-5bMn\left(\left(\frac{\beta_2(M-2n)}{n}+1\right)^2-1\right)\left(\frac{\beta_2(M-2n)}{n}+1\right)
\end{array}
\right) .
\tag{30}
$$

$$
\begin{aligned}
B_4 &= -\frac{(M-2n)^2}{n^3}\big(k\log_{\mathrm{e}} 2\cdot M^2+2Mn^2-4k\log_{\mathrm{e}} 2\cdot Mn \\
&\qquad\qquad\qquad\qquad\qquad + 4k\log_{\mathrm{e}} 2\cdot n^2\big) \ , \\
B_3 &= -\frac{(M-2n)}{n^2}\big(-M^2n+4k\log_{\mathrm{e}} 2\cdot M^2+6Mn^2 \\
&\qquad\qquad - 16k\log_{\mathrm{e}} 2\cdot Mn+16k\log_{\mathrm{e}} 2\cdot n^2\big) \ , \\
B_2 &= -\frac{3kM^2\log_{\mathrm{e}}2+4Mn^2-16kMn\log_{\mathrm{e}}2+20kn^2\log_{\mathrm{e}}2}{n} \ , \\
B_1 &= 4k\log_{\mathrm{e}} 2\cdot n \ .
\end{aligned}
$$

Note that $\beta_2 > 1$ and it holds that $A_1 \le (B_4+B_3)\beta_2^3 + B_2\beta_2^2 + B_1\beta_2$ for $B_4 \le 0$. In addition, $m > 2n$. Moreover, the following inequality holds:

$$
\begin{aligned}
B_4+B_3 &= -\frac{M^2-4n^2}{n^3}\big(k\log_{\mathrm{e}} 2\cdot M^2+Mn^2 \\
&\qquad\qquad - 4k\log_{\mathrm{e}} 2\cdot Mn+4k\log_{\mathrm{e}} 2\cdot n^2\big) \\
&= -\frac{M^2-4n^2}{n^3}\big(k(M^2-4Mn+4n^2)+Mn^2\big)\log_{\mathrm{e}} 2 \\
&\le 0 \ .
\end{aligned}
$$

Therefore, we have $A_1 \le (B_4+B_3+B_2+B_1)\beta_2 = \beta_2\sum_{i=1}^{4} B_i$. In other words, $A_1 \le 0$ if $\sum_{i=1}^{4} B_i \le 0$. With some manipulations we obtain

$$
\sum_{i=1}^{4} B_i = -\frac{M^2\left(k\log_{\mathrm{e}}2\,(M-3n)\,(M-n)+Mn^2\right)}{n^3} \ . \tag{32}
$$

To show $\sum_{i=1}^{4} B_i \le 0$, we in the following consider two cases depending on whether or not $M-3n \ge 0$.

When $M\geq 3n$, it is actually easy to show that $\sum_{i=1}^{4} B_i \leq 0$. In the case in which $M<3n$, it is clear that $\sum_{i=1}^{4} B_i < 0$ if $\frac{mn}{\log_{\rm e} 2\cdot(M-n)(3n-M)} > \frac{k}{n}$, which holds due to the following:

Assume that $\frac{mn}{\log_{\rm e} 2\cdot(M-n)(3n-M)} > \frac{k}{n}$ does not hold under the condition $M<3n$. Then, we have

$$C(\gamma_{\rm T,2}) - \frac{k}{n} < \frac{\log_{\rm e}2\cdot(M-n)(3n-M)-Mn}{\log_{\rm e}2\cdot(M-n)(3n-M)} < 0\ . \tag{33}$$

Note that the error probability of each link is lower than 10^{-1}, i.e., we have $\varepsilon_i \leq 10^{-1} \leq \frac{1}{2}$. This reliability constraint implies that the coding rate is lower than the Shannon capacity of each link, i.e., $C(\gamma_{\rm T,2})-\frac{k}{n} > 0$ which contradicts (33) hence the assumption of $\frac{mn}{\log_{\rm e} 2\cdot(M-n)(3n-M)} > \frac{k}{n}$ is not true. As a result, $A_1 \leq 0$ holds for all possible values of n and M under the conditions that $2n<m$ and $\beta_2>1$.

Next, we have $A_2 = D_6\beta_2^6 + D_5\beta_2^5 + D_4\beta_2^4 + D_3\beta_2^3 + D_2\beta_2^2$, where

$$\begin{aligned}
D_6 &= -\frac{(M-2n)^6}{n^4} \leq 0\ ,\\
D_5 &= -\frac{(M-2n)^4\left(27M-54n+8Mn\right)}{4n^3} \leq 0\ ,\\
D_4 &= -\frac{(M-2n)^2}{4n^2}\big(32M^2n+75M^2\\
&\qquad\qquad -64Mn^2-308Mn+268n^2\big)\ ,\\
D_3 &= \frac{6M^2\left(M-2n\right)}{n} - 10M(M-2n)^2\\
&\quad -\frac{15M(M-2n)^2}{n} - \frac{18(M-2n)^3}{n}\\
&\leq 0\ ,\\
D_2 &= -4M^2n - 20M^2 + 8Mn^2 + 48Mn - 28n^2 \leq 0\ .
\end{aligned}$$

Note that $M\geq 2n$, it is easy to show that $D_i\leq 0, i=6,5,3,2$. Similar to the discussion regarding (32), it is easy to show $\sum_{i=4}^{6} D_i \leq 0$. As $\beta_2\geq 1$, we have $0 \geq (D_6+D_5+D_4)\beta_2^6 \geq D_6\beta_2^6 + D_5\beta_2^5 + D_4\beta_2^4$. Note that $D_3\beta_2^3 \leq 0$ and $D_2\beta_2^2 \leq 0$. As a result, we have $A_2 \leq 0$.

Combining $A_1\leq 0$ and $A_2 \leq 0$, we have

$$\frac{\partial^2 w_{\rm T,2}}{\partial n^2} = \sqrt{\frac{n}{V(\gamma_{\rm T,2})}}\left(A_1 + A_2 + A_3(C(\gamma_{\rm T,2}) - r)\right) \leq 0\ . \tag{34}$$

According to (25), we have $\frac{\partial^2 \varepsilon_{\rm T,2}}{\partial v^2} \geq 0$. Finally, we obtain $\frac{\partial^2 \varepsilon_{\rm T}}{\partial v^2} \approx \frac{\partial^2 \varepsilon_{\rm T,1}}{\partial v^2} + \frac{\partial^2 \varepsilon_{\rm T,2}}{\partial v^2} \geq 0$.

Appendix C
Proof of Proposition 3

When v is fixed, i.e., $v=v_0$ and v_0 is a constant, the SNR in the second hop becomes $\gamma_{\rm PT,2} = \beta_2(\frac{2v_0}{M-v_0}+\rho) = \beta_2(u\rho+\rho) = \beta_{\rm P,2}\rho$, where $u=\frac{2v_0}{M-v_0}$ and $\beta_{\rm P,2} = \rho(1+u)\beta_2$. Now the SNRs in each hop under the PT-S protocol for a fixed $v=v_0$ are identical to the SNRs under the PS protocol. It is also obvious that the constraint $\gamma_{\rm P,2}\geq 1$ still holds for $\beta_{\rm P,2} > \beta_2$. Thus, the proof of Proposition 1 can be directly applied to prove Proposition 3.

When ρ is fixed, i.e., $\rho=\rho_0$, the SNR in the first hop becomes $\gamma_{\rm PT,1} = \beta_1(1-\rho_0) = \beta_{\rm T,1}$. Then, the

SNR in the second hop is given by

$$\begin{aligned}\gamma_{\text{PT},2} &= \beta_2\Big(\frac{v}{M-v}+\rho_0\Big)\\ &= \beta_2\Big(\frac{v}{M-v}+K\frac{v}{M-v}\Big)\\ &= \beta_{\text{T},2}\Big(\frac{v}{M-v}\Big)\ ,\end{aligned} \tag{35}$$

where $K=\frac{(M-v)\rho}{v}$ and $\beta_{\text{T},2}=(1+K)\beta_2$. The SNR in each hop under the PT-S protocol for a fixed $\rho=\rho_0$ is identical to the corresponding SNRs under the TS protocol. Thus, the proof of Proposition 2 can also be directly applied to for Proposition 3.

APPENDIX D
PROOF OF PROPOSITION 4

First, the proof of Proposition 1 is based on the assumption that blocklengths of the two relaying hops are fixed (regardless of whether they have an equal length or not). Therefore, this proof also holds for the first statement of Proposition 4, i.e., for a given n_1, $\varepsilon_{\text{P},1}$, $\varepsilon_{\text{P},2}$ and $\varepsilon_{\text{P,O}}\approx\varepsilon_{\text{P},1}+\varepsilon_{\text{P},2}$ are convex in ρ, $\rho\in(0,1)$.

In addition, for the second statement of Proposition 4, where ρ is given, by substituting n_1 for v, the proof of Proposition 2 also holds. In particular, the SNRs under the PS protocol with the joint design in the first and second hops are $\gamma_{\text{P},1}=\beta_{\text{P},1}$ and $\gamma_{\text{P},2}=\beta_{\text{P},2}(\frac{v}{M-v})$, i.e., they share the same analytic form with the SNRs under the TS protocol. Therefore, proof of Proposition 2 also holds, i.e., the second derivative of $\varepsilon_{\text{P,O}}$ with respect to n_1 is non-negative.

APPENDIX E
PROOF OF PROPOSITION 5

When n_1 is given, $\varepsilon_{\text{T},1}$ is not influenced by v, i.e., $\frac{\partial^2\varepsilon_{\text{T},1}}{\partial v^2}=0$. Note that $v=M-n_1-n_2$ where M and n_1 are fixed. Based on (26) and (34), it can be easily shown that $\frac{\partial^2\varepsilon_{\text{T},2}}{\partial v^2}=\frac{\partial^2\varepsilon_{\text{T},2}}{\partial n_2^2}\geq 0$. Hence, $\frac{\partial^2\varepsilon_{\text{T,O}}}{\partial v^2}\geq 0$ and $\varepsilon_{\text{T,O}}$ is convex in v for a given n_1.

In the other case, v is given as v_0. In the following, we show the second order derivatives of $\varepsilon_{\text{T},i}, i=1,2$ in n_1 are non-negative. In this case, the SNR in the second hop is:

$$\gamma_{\text{T},2}=\beta_2\frac{v_0}{M-v_0-n_1}=\beta_2'\frac{1}{(M_0-n_1)}\ , \tag{36}$$

where $\beta_2'=\beta_2 v_0$ and $M_0=M-v_0$. Recall that $\varepsilon_{\text{T},i}=Q(w_{\text{T},i})$. In the following, we start with the relationship between $w_{\text{T},2}$ and $w_{\text{T},1}$ with n_1. The second derivative of $w_{\text{T},2}$ to n_1 is given by

$$\frac{\partial^2 w_{\text{T},2}}{\partial n_1^2}=\sqrt{\frac{M_0-n_1}{V(\gamma_{\text{T},2})}}\left[A_1'+A_2'\left(C(\gamma_{\text{T},2})-\frac{k}{(M_0-n_1)}\right)\right]\ , \tag{37}$$

where

$$\begin{aligned}A_1' &= G_4\beta_2'^4+G_3\beta_2'^3+G_2\beta_2'^2\ ,\\ A_2' &= H_6\beta_2'^6+H_5\beta_2'^5+H_4\beta_2'^4+H_3\beta_2'^3+H_2\beta_2'^2\\ &\qquad +H_1\beta_2'^1+H_0\beta_2'^0\ ,\end{aligned}$$

in which

$$
\begin{aligned}
&G_4 = -k\log_e 2,\\
&G_3 = (M_0-n_1)^2 - 4k\log_e 2(M_0-n_1)\ ,\\
&G_2 = -3k\log_e 2(M_0-n_1)^2\ ,\\
&H_6 = -3(M_0-n_1)^4 - 4\ ,\\
&H_5 = -18(M_0-n_1)^5 - 24(M_0-n_1)\ ,\\
&H_4 = -45(M_0-n_1)^6 - 6(M_0-n_1)^4 - 56(M_0-n_1)^2\ ,\\
&H_3 = -60(M_0-n_1)^7 - 12(M_0-n_1)^5 - 72(M_0-n_1)^3\ ,\\
&H_2 = -45(M_0-n_1)^8 - 51(M_0-n_1)^4\ ,\\
&H_1 = -18(M_0-n_1)^9 + 12(M_0-n_1)^7 + 6(M_0-n_1)^5\ ,\\
&H_0 = -\left(3(M_0-n_1)^{10} - 6(M_0-n_1)^8 + 3(M_0-n_1)^6\right)\ .
\end{aligned}
$$

We first discuss A'_1. Note that $\beta'_2 > 1$, and we have that $A'_1 \leq (G_4+G_3)\beta'^3_2 + G_1\beta'^2_2$ for $G_4 \leq 0$. It also holds that $G_4+G_3+G_2 = -k\log_e 2 + (M_0-n_1)^2 - 4k\log_e 2(M_0-n_1) - 3k\log_e 2(M_0-n_1)^2 \leq 0$. Hence, we have $A'_1 \leq G_4+G_3+G_2 \leq 0$.

In addition, it is clear that $H_i < 0\ \forall\ i = 0,1,...,6$ and $n_2 = (M_0-n_1) \in \mathbb{Z}^+$. Therefore, we can show $A'_2 < 0$ similarly. Then, we have $\frac{\partial^2 W_{\mathrm{T},2}}{\partial n_1^2} < 0$ as $A'_1 \leq 0$ and $A'_2 < 0$. Hence, we have $\frac{\partial^2 \varepsilon_{\mathrm{T},2}}{\partial n_1^2} \geq 0$, according to (25). In addition, from (26), we have $\frac{\partial^2 \varepsilon_{\mathrm{T},1}}{\partial n_1^2} \geq 0$. Therefore, $\frac{\partial^2 \varepsilon_{\mathrm{T,O}}}{\partial n_1^2} \geq 0$ and thus, $\varepsilon_{\mathrm{T,O}}$ is convex in n_1 for a given v.

Appendix F
Proof of Proposition 6

When v and ρ are fixed, according to Appendix E, $\varepsilon_{\mathrm{PT},1}$, $\varepsilon_{\mathrm{PT},2}$ and $\varepsilon_{\mathrm{PT,O}}$ are convex in n_1. Subsequently, when v and n_1 are fixed, the convexity of $\varepsilon_{\mathrm{PT},1}$, $\varepsilon_{\mathrm{PT},2}$ and $\varepsilon_{\mathrm{PT,O}}$ in ρ is confirmed by the proof in Appendix A. Finally, when ρ and n_1 are fixed, the proof in Appendix B holds for showing the convexity of $\varepsilon_{\mathrm{PT},1}$, $\varepsilon_{\mathrm{PT},2}$ and $\varepsilon_{\mathrm{PT,O}}$ in v.

References

[1] C. She, C. Yang and T. Q. S. Quek, "Radio resource management for ultra-reliable and low-latency communications," *IEEE Commun. Mag.*, vol. 55, no. 6, pp. 72-78, Jun. 2017.

[2] Y. Hu, M. C. Gursoy and A. Schmeink, "Relaying-Enabled Ultra-Reliable Low Latency Communications in 5G", *IEEE Network*, vol. 32, no. 2, pp. 62-68, Mar.-Apr. 2018.

[3] 3GPP, "Study on Scenarios and Requirements for Next GenerationAccess Technologies," *Tech. Spec. Group Radio Access Network, tech.* rep. 38.913, Release 14, Oct. 2016.

[4] S. C. Lin and K. C. Chen, "Statistical QoS control of network coded multipath routing in large cognitive machine-to-machine networks," *IEEE Internet Things J.*, vol. 3, no. 4 pp. 619-627, Aug. 2016.

[5] P. Kamalinejad *et al.*, "Wireless energy harvesting for the Internet of Things," *IEEE Commun. Mag.*, vol. 53, no. 6, pp. 102-108, June 2015.

[6] M. L. Ku, W. Li, Y. Chen, and K. J. R. Liu, "On energy harvesting gain and diversity analysis in cooperative communications," *IEEE J. Select. Area Commun.*, vol. 33, no. 12, pp. 2641–2657, Dec. 2015.

[7] S. Bi, C. K. Ho, and R. Zhang, "Wireless powered communication: Opportunities and challenges," *IEEE Commun. Mag.*, vol. 53, no. 4, pp. 117–125, Apr. 2015.

[8] X. Lu, P. Wang, D. Niyato, D. I. Kim and Z. Han, "Wireless Networks With RF Energy Harvesting: A Contemporary Survey," *IEEE Commun. Surveys & Tuts.*, vol. 17, no. 2, pp. 757-789, Secondquarter 2015.

[9] B. Makki, T. Svensson, K. Buisman, J. Perez and M. S. Alouini, "Wireless Energy and Information Transmission in FSO and RF-FSO Links," *IEEE Commn. Lett.*, vol. 7, no. 1, pp. 90-93, Feb. 2018.

[10] X. Zhou, R. Zhang, and C. K. Ho, "Wireless information and power transfer: Architecture design and rate-energy tradeoff," *IEEE Trans. Wireless. Commn.*, vol. 61, no. 11, pp. 4754–4767, Nov. 2013.

[11] A. A. Nasir, X. Zhou, S. Durrani, and R. A. Kennedy, "Relaying protocols for wireless energy harvesting and information processing," *IEEE Trans. Wireless. Commn.*, vol. 12, no. 7, pp. 3622–3636, Jul. 2013.

[12] H. Chen, Y. Li, Y. Jiang, Y. Ma and B. Vucetic, "Distributed power splitting for SWIPT in relay interference channels using game theory," *IEEE Trans. Wireless. Commn.*, vol. 14, no. 1, pp. 410-420, Jan. 2015.

[13] M. Haghifam, B. Makki, M. Nasiri-Kenari and T. Svensson, "On joint energy and information transfer in relay networks with an imperfect power amplifier," *IEEE PIMRC*, Valencia, 2016, pp. 1-6.

[14] I. Krikidis, "Simultaneous information and energy transfer in large-scale networks with/without relaying," *IEEE Trans. Wireless. Commn.*, vol. 62, no. 3, pp. 900–912, Mar. 2014.

[15] M. Haghifam, B. Makki, M. Nasiri-Kenari, T. Svensson, "On Wireless Energy and Information Transfer in Relay Networks." arXiv:1607.07087, Jul. 2016

[16] Y. Polyanskiy, H. Poor, and S. Verdu, "Channel coding rate in the finite blocklength regime," *IEEE Trans. Inf. Theory*, vol. 56, no. 5, pp. 2307–2359, May 2010.

[17] Y. Polyanskiy, H. Poor, and S. Verdu, "Dispersion of the Gilbert-Elliott channel," *IEEE Trans. Inf. Theory*, vol. 57, no. 4, pp. 1829–1848, April 2011.

[18] W. Yang, G. Durisi, T. Koch and Y. Polyanskiy "Quasi-static multiple-antenna fading channels at finite blocklength," *IEEE Trans. Inf. Theory*, vol. 60, no. 7, July 2014.

[19] G. Ozcan and M. C. Gursoy, "Throughput of cognitive radio systems with finite blocklength codes," *IEEE J. Select. Area Commun.*, vol. 31, no. 11, pp. 2541-2554, Nov. 2013.

[20] Y. Hu, J. Gross and A. Schmeink, "On the capacity of relaying with finite blocklength," *IEEE Trans. Veh. Technol.*, vol. 65, no. 3, pp. 1790–1794, Mar. 2016.

[21] Y. Hu, J. Gross and A. Schmeink, "On the performance advantage of relaying under the finite blocklength regime," *IEEE Commn. Lett.*, vol. 19, no. 5, pp. 779 - 782, May 2015.

[22] Y. Hu, A. Schmeink and J. Gross "Blocklength-limited performance of relaying under quasi-static Rayleigh channels," *IEEE Trans. Wireless. Commn.*, vol. 15, no. 7, pp. 4548 - 4558, Jul. 2016.

[23] J. Yang, "Achievable rate for energy harvesting channel with finite blocklength," in *IEEE ISIT.*, Jun. 2014, pp. 811–815.

[24] A. Guo, H. Yin and W. Wang, "Performance Analysis of Energy Harvesting Wireless Communication System With Finite Blocklength," *IEEE Commn. Lett.*, vol. 20, no. 2, pp. 324-327, Feb. 2016.

[25] O. L. A. Lopez, E. M. G. Fernandez, H. Alves, et al., "Wireless powered communications with finite battery and finite blocklength," *IEEE Trans. Commn.*, vol. PP, no. 99, pp. 1-1. Dec. 2017

[26] B. Makki, T. Svensson and M. Zorzi, "Wireless Energy and Information Transmission Using Feedback: Infinite and Finite Block-Length Analysis," *IEEE Trans. Commn.*, vol. 64, no. 12, pp. 5304-5318, Dec. 2016.

[27] T. A. Khan, R. W. Heath and P. Popovski, "Wirelessly Powered Communication Networks With Short Packets," *IEEE Trans. Commn.*, vol. 65, no. 12, pp. 5529-5543, Dec. 2017.

[28] O. L. A. Lopez, H. Alves, R. D. Souza, et al., "Ultra reliable short message relaying with wireless power transfer," in *IEEE ICC*, Paris, France, 21-25 May 2017

[29] M. Haghifam, B. Makki, M. Nasiri-Kenari, T. Svensson, M. Zorzi, " Wireless-powered relaying with finite block-length codes", arXiv:1611.05995v1, Nov. 2016.

[30] Z. Ding, S. M. Perlaza, I. Esnaola, and H. V. Poor, "Power allocation strategies in energy harvesting wireless cooperative networks," *IEEE Trans. Wireless. Commn.* vol. 13, no. 2, pp. 846–860, 2014.

[31] M. Peng, Y. Liu, D. Wei, W. Wang, and H.-H. Chen, "Hierarchical cooperative relay based heterogeneous networks," *IEEE Wireless Commun.*, vol. 18, no. 3, pp. 48–56, Jun. 2011.

[32] G. Scutari, F. Facchinei and L. Lampariello, "Parallel and distributed methods for constrained nonconvex optimization—Part I: Theory," *IEEE Trans. on Sig. Proc.*, vol. 65, no. 8, pp. 1929-1944, Apr. 2017.

[33] B. Clerckx, "Wireless Information and Power Transfer: Nonlinearity, Waveform Design and Rate-Energy Tradeoff", *IEEE Trans. on Sig. Proc.*, vol 66, no 4, pp 847-862, Feb. 2018.

[34] B. Clerckx, R. Zhang, R. Schober, D. Wing Kwan Ng, D. In Kim, H. Vincent Poor "Fundamentals of Wireless Information and Power Transfer: From RF Energy Harvester Models to Signal and System Designs" *arXiv:1803.07123*, Mar. 2018

[35] J. M. Kang, I. M. Kim, and D. I. Kim, "Wireless Information and Power Transfer: Rate-Energy Tradeoff for Nonlinear Energy Harvesting," *IEEE Trans. Wireless Commun.*, vol. 17, pp. 1966-1981, Mar. 2018.

[36] M. Varasteh, B. Rassouli, and B. Clerckx, "On Capacity-Achieving Distributions Over Complex AWGN Channels Under Nonlinear Power Constraints and their Applications to SWIPT," *arXiv:1712.01226*, Dec. 2017.

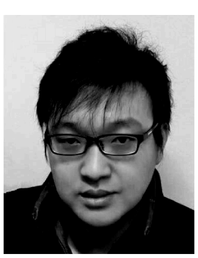

Yulin Hu received his M.Sc.E.E degree from USTC, China, in 2011. He successfully defended his dissertation of a joint Ph.D. program supervised by Prof. Anke Schmeink at RWTH Aachen University and Prof. James Gross at KTH Royal Institute of Technology in Dec. 2015 and received his Ph.D.E.E. degree (Hons.) from RWTH Aachen University where he was a Research Fellow since Jan. to Dec. in 2016. Since 2017, he works as a senior researcher and project lead in ISEK research group at RWTH Aachen University. From May to July in 2017, he was a visiting scholar with Prof. M. Cenk Gursoy in Syracuse University, USA. His research interests are in information theory, optimal design of wireless communication systems. He has been invited to contribute submissions to multiple conferences. He was a recipient of the IFIP/IEEE Wireless Days Student Travel Awards in 2012. He received the Best Paper Awards at IEEE ISWCS 2017 and IEEE PIMRC 2017, respectively. He is currently serving as an editor for Physical Communication (Elsevier).

Yao Zhu received the B.S. degree in electrical engineering from University Bremen, Bremen, Germany, in 2015, the Master's degree in Information Technology and Computer Engineering from RWTH Aachen University, Aachen, Germany in 2018. He is currently working toward the Ph.D. degree with the ISEK Research Group, RWTH Aachen, Germany. His research interest includes ultra-reliable and low-latency communication and mobile edge networks.

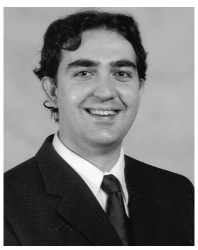

M. Cenk Gursoy received the B.S. degree with high distinction in electrical and electronics engineering from Bogazici University, Istanbul, Turkey, in 1999 and the Ph.D. degree in electrical engineering from Princeton University, Princeton, NJ, in 2004. He was a recipient of the Gordon Wu Graduate Fellowship from Princeton University between 1999 and 2003. Between 2004 and 2011, he was a faculty member in the Department of Electrical Engineering at the University of NebraskaLincoln (UNL). He is currently a Professor in the Department of Electrical Engineering and Computer Science at Syracuse University. His research interests are in the general areas of wireless communications, information theory, communication networks, and signal processing. He is currently a member of the editorial boards of IEEE Transactions on Wireless Communications, IEEE Transactions on Green Communications and Networking, IEEE Transactions on Communications, IEEE Transactions on Vehicular Technology. He also served as an editor for IEEE Transactions on Wireless Communications between 2010 and 2015, IEEE Communications Letters between 2012 and 2014, IEEE Journal on Selected Areas in Communications - Series on Green Communications and Networking (JSAC-SGCN) between 2015 and 2016, and Physical Communication (Elsevier) between 2010 and 2017. He was a Co-Chair of the Communication QoS and System Modeling Symposium, 2017 International Conference on Computing, Networking and Communications (ICNC). He received an NSF CAREER Award in 2006. More recently, he received the EURASIP Journal of Wireless Communications and Networking Best Paper Award, 2017 IEEE PIMRC Best Paper Award, 2017 IEEE Green Communications & Computing Technical Committee Best Journal Paper Award, UNL College Distinguished Teaching Award, and the Maude Hammond Fling Faculty Research Fellowship. He is a Senior Member of IEEE, and is the Aerospace/Communications/Signal Processing Chapter Co-Chair of IEEE Syracuse Section.

Anke Schmeink received the Diploma degree in mathematics with a minor in medicine and the Ph.D. degree in electrical engineering and information technology from RWTH Aachen University, Germany, in 2002 and 2006, respectively. She worked as a research scientist for Philips Research before joining RWTH Aachen University in 2008 where she is an associate professor since 2012. She spent several research visits with the University of Melbourne, and with the University of York. Anke Schmeink is a member of the Young Academy at the North Rhine-Westphalia Academy of Science. Her research interests are in information theory, systematic design of communication systems and bioinspired signal processing.